Effects of low-energy electron and ion irradiation on CO/Cu(100): *In-situ* production and coadsorbate-induced adsorption of CO above room temperature

H. Yu, D. Q. Hu,[a] and K. T. Leung[b]
Department of Physics and Department of Chemistry, The University of Waterloo, Waterloo, Ontario N2L 3G1, Canada

(Received 3 January 1997; accepted 16 May 1997)

The surface reactions of CO with clean, oxygen-precovered and carbon-precovered surfaces of Cu(100) assisted by low-energy electron or ion irradiation were investigated using high-resolution electron energy loss spectroscopy and temperature programmed desorption mass spectrometry. We observed an anomalous adsorption of ''stabilized'' CO species on Cu(100) above room temperature that were produced *in situ* by low-energy electron irradiation of CO/Cu(100) at 120 K and by low-energy ion irradiation of Cu(100) in CO or with pre- or postexposure of O_2 in C_2H_4 at room temperature. The corresponding C–O stretch vibration was found to be redshifted by 73 cm^{-1} from its nominal position (2084 cm^{-1}) at 120 K. Furthermore, unlike the normal C–O stretch that could only be observed below 200 K, the redshifted peak could be found up to 420 K. From the different mechanisms that could cause the observed redshift and stabilization effects, we propose a direct-interaction bonding model involving a ''tilted'' CO molecule on an atop site semibridge bonded to an O atom in a four-fold hollow site. Other processes such as reaction activation and creation of defect sites as well as sputtering effects induced by low-energy electron or ion irradiation are discussed. [S0734-2101(97)01905-2]

I. INTRODUCTION

The chemisorption of CO on Cu(100) has been the subject of many intense investigations in surface science over the past twenty years. Previous studies[1–3] showed that CO adsorbs on the atop site of the Cu(100) surface with a $c(2\times2)$ low-energy electron diffraction (LEED) structure[4] at low temperature (<200 K). Furthermore, the frequencies cited in the literature for both the Cu–CO [or ν(Cu–CO)] stretch at 342 cm^{-1} and the C–O [or ν(C–O)] stretch at 2089 cm^{-1} were found to be nearly independent of the coverage. The commonly accepted bonding model is obtained from metal-carbonyl chemistry and it involves the interplay between the dative σ donation from CO to a substrate metal atom and back donation from the *d* orbitals of the metal atom to the $2\pi^*$ orbital of CO. To date, no CO has been found to adsorb on a clean or oxidized Cu(100) surface at room temperature (RT), although the adsorption of molecules containing the CO functional group, such as alkoxides, on Cu(100) above RT was reported by Sexton.[5]

The use of low-energy electron or ion beam irradiation has become an increasingly powerful tool for the development of new materials.[6] Electron/ion irradiation (EII), in particular, has been used to produce reactive ions and free radicals on surfaces and to provide new synthetic routes involving gas-surface reactions instead of thermal chemistry. For example, atomic nitrogen could be obtained by using electron dissociation of N_2 and was found to adsorb on Cu(100) at RT.[7] In addition to reaction activation, EII could, depending on the impact energy (IE) of the charged particle beam, also introduce other effects such as adsorbate removal (as in electron-stimulated desorption and ion sputtering) and creation of surface defect sites, which might affect the subsequent reaction processes and adsorption properties. In the case of ion irradiation, ion implantation and bulk atomic displacement (i.e., creation of bulk defects) could also occur. As in many applications in materials processing that involve film growth and surface modification by EII,[8] these processes occur concurrently with the reaction activation process, making the study of an isolated chemical reaction difficult. Despite the many technological interests in the effects induced by EII, there is virtually no fundamental information about these effects. Most studies have thus far focused on parameter optimization in the engineering of various novel materials involving EII. Since many important reactions induced by low-energy EII remain unknown, it would therefore be of practical interest to investigate the fundamental mechanisms that control the initial adsorption and subsequent surface reactions induced by EII.

In the present work, we study these EII-induced effects for the aforementioned model chemisorption system, CO/Cu(100). In particular, we investigate the adsorption properties induced by low-energy EII for CO on clean, oxygen-precovered and carbon-precovered surfaces of Cu(100) by using high-resolution electron energy loss spectroscopy (EELS) and temperature programmed desorption (TPD) mass spectrometry. We show that ''stabilized'' CO adsorption can be obtained at RT by using low-energy EII of CO on clean Cu(100) or ethylene (C_2H_4) on Cu(100) with pre- or postexposure of O_2. The ''stabilized'' CO adsorption is

[a]Present address: Hewlett-Packard Company, 1000 NE Circle Blvd., MS 5UP4, Corvallis, OR 97330.
[b]Author to whom correspondence to the Dept. of Chemistry should be made; Electronic mail:tong@uwaterloo.ca

characterized by an ''anomalous'' redshift of 73 cm^{-1} in the ν(C–O) stretching frequency obtained at low temperature, and is found to be stable to as high as 420 K. By examining the effects generated by different conditions of EII and the plausible mechanisms of coadsorption, we propose a direct-interaction model involving an O–CO complex in order to explain the observed redshift in ν(C–O) and the unusual stabilization effects of CO/Cu(100) at RT.

II. EXPERIMENTAL METHOD

Our experiments were performed in a home-built ultrahigh vacuum chamber with a base pressure of better than 1×10^{-10} Torr. Our chamber was equipped with an ion (-sputtering) gun, a four-grid retarding-field optics for both LEED and Auger electron spectroscopic (AES) analyses, a quadrupole mass spectrometer (QMS) for TPD studies, and a home-built EELS spectrometer.[9] The QMS was housed in a separate chamber that was differentially pumped by a 60 ℓ/s ion pump. The only entrance to the QMS in this chamber was provided by a 2-mm-diam orifice located approximately 10 mm from the ionizer region. This arrangement was found to be effective in preventing the desorbed species in the surrounding from entering the ionizer region. During the TPD experiments, the front face of the crystal was positioned less than 0.5 mm from the orifice and the temperature was varied at a linear heating rate of 1 K/s with a precision of better than $\pm$ 1 K. The Cu(100) sample (9.5 mm diameter $\times$ 2 mm thick) with a stated purity of 99.999% was purchased from Monocrystals Company. The sample was cleaned by repeated cycles of Ar^+ sputtering [at 500 eV (IE) and 10 mA (electron emission current) under an ambient Ar pressure of 2×10^{-5} Torr for 30 minutes] and annealing to 800 K, until a sharp 1×1 LEED pattern and no detectable Auger peaks attributable to such impurities as C, O or S were obtained. The surface temperature of the sample was monitored by a type K thermocouple (mechanically fastened to the front face of the sample) to an absolute accuracy of $\pm$ 20 K. All the exposures were performed using variable leak valves, with the pressure monitored by an uncalibrated ionization gauge. Unless stated otherwise, electron irradiation was accomplished by bombarding the sample with electrons thermionically emitted from a heated tungsten filament, positioned 40 mm from the sample, at an electron flux of ~2.7 $\mu A/mm^2$. Ion irradiation was performed by operating the ion gun at an ambient (CO or C_2H_4) gas pressure of 1×10^{-6} Torr with an ion flux of ~10 nA/mm^2. The gaseous samples, CO and C_2H_4, both of 99.99% purity, were purchased from Matheson and used without further purification. The IE of the electron or ion beam could be controlled by adjusting the floating voltage applied to the sample with respect to a pre-selected beam voltage of the ion gun.

In the past two decades, high-resolution EELS has become an increasingly important tool for surface analysis, with the energy resolution of the state-of-the-art spectrometers reaching the sub-meV level, i.e., below 4 cm^{-1} (or 0.5 meV) full width at half maximum (FWHM).[10] Most of these spectrometers are, however, specially designed to probe surface vibrations using a low impact energy, which limits their applications for other types of experiments. We have recently developed a multitechnique portable analyzer for both low-impact-energy applications (as in surface vibrational spectroscopy) and high-impact-energy work (including investigations of electronic transitions and other phenomena). A schematic diagram of our EELS spectrometer is shown in Fig. 1. The analyzer and the monochromator are mountable separately on 8-inch conflat flanges, which make them portable from one chamber to another. Both the monochromator and the analyzer are based on an identical electron optical design, which consists of a 51-mm-mean-radius hemispherical deflector (HD) coupled with a cylindrical double retardation lens (DRL) system.[9] The analyzer system is mounted on a single-axis goniometer and can be rotated around an axis perpendicular to the dispersion plane of the analyzer, hence making it suitable for angle-resolved experiments.

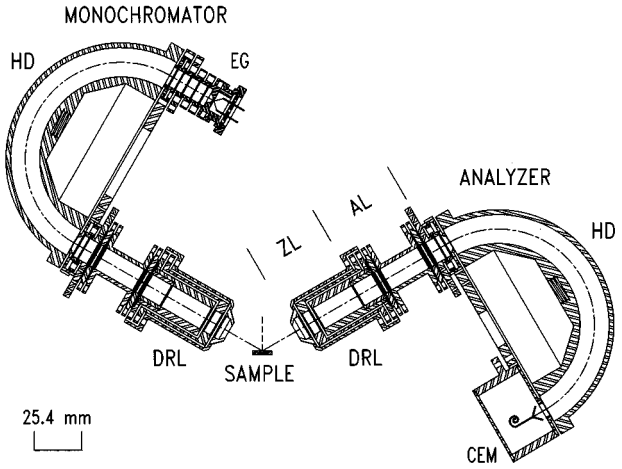

FIG. 1. Schematic diagram of the electron energy loss spectrometer at the University of Waterloo. EG: electron gun; HD: hemispherical deflector; DRL: double retardation lens; ZL: zoom lens; AL: afocal lens, CEM: channel electron multiplier.

The DRL system is capable of decelerating (and accelerating) electrons over a wide dynamic range of kinetic energy (up to a factor of 1000), which enables the spectrometer to be used for different types of experiments that involve the analysis of electrons in a wide energy range. This compound lens system can be divided into two elemental lenses: a three-element zoom lens (ZL) and a five-element afocal lens (AL), with a common electrode acting as a dividing aperture between the two elemental lenses.[11] When the analyzer is operated in the constant-absolute-resolution mode (i.e., with a fixed pass energy), the DRL is operated in a double focusing mode. As a first step in the initial optics optimization procedure, the five-element AL is used to provide a high retardation ratio while the three-element ZL serves as an Einzel lens. The desired kinetic energy range can then be scanned by keeping the retardation ratio of the AL fixed while varying that of the three-element ZL with respect to the scanning voltage, which results in an appropriate change in the overall retardation ratio of the entire seven-element DRL. In order to minimize the variation in the overall trans-

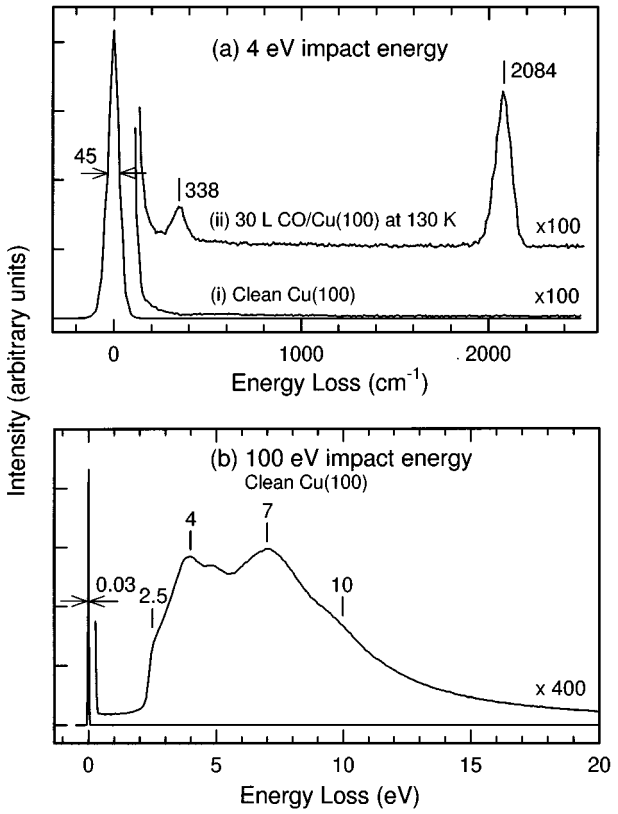

FIG. 2. Typical electron energy loss spectra for (a) a clean Cu(100) surface with (ii) and without (i) a 30 L exposure of CO at 130 K collected at 4 eV impact energy, and for (b) a clean Cu(100) surface recorded at 100 eV impact energy over an extended energy loss range illustrating the onset of the electronic band structure.

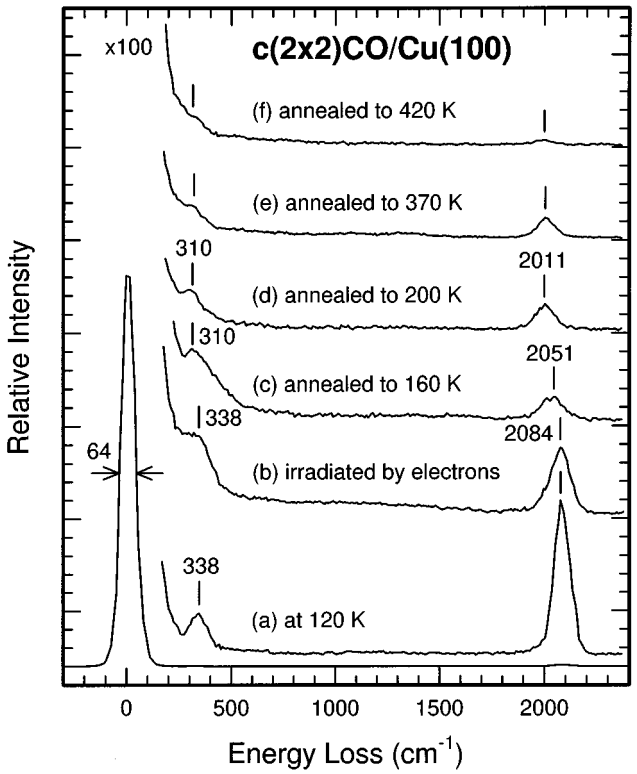

FIG. 3. Vibrational electron energy loss spectra for (a) 100 L of CO adsorbed on Cu(100) at 120 K, and (b) sample (a) irradiated with electrons at 100 eV and 2.7 μA/mm^2 for 10 minutes at 120 K, followed by annealing to (c) 160, (d) 200, (e) 370, and (f) 420 K.

mission function of the DRL while scanning over a wide dynamic range of electron energy, only the voltage of the second element in the three-element ZL needs to be adjusted simultaneously to maintain an intermediate image at the center of the dividing aperture. The DRL system can also be operated in a single focusing mode, which facilitates an acceptance half-angle of smaller than 1.0°. This mode is particularly useful in angle-resolved experiments that require an angular resolution better than the nominal resolution of 1.5° half-angle.

To illustrate the typical performance attainable by our spectrometer, we show both the high-resolution and extended-range EELS spectra for a Cu(100) sample in Fig. 2. The high-resolution EELS spectrum of CO/Cu(100) in Fig. 2(a) clearly shows two prominent peaks at 338 cm^{-1} and 2084 cm^{-1}, which are in good accord with, respectively, the ν(Cu–CO) and ν(C–O) frequencies reported previously.[1–3] In Fig. 2(b), the energy loss features of Cu(100) at 2.5 eV, 4 eV and 10 eV can be assigned to interband transitions originating from the Cu d band while the feature at 7 eV corresponds to a bulk plasmon excitation.[12] In the high-resolution mode, our spectrometer is capable of an optimal energy resolution of 45 cm^{-1} FWHM, with a count rate of 100 kHz for the elastic peak, at a typical (low) impact energy of 4 eV [Fig. 2(a)]. In the high impact energy mode (e.g., 100 eV), the energy resolution becomes 0.03 eV FWHM [Fig. 2(b)], which is considerably better than the performance of commercially available spectrometers. Our spectrometer therefore offers adequate performance for most of our applications ranging from the present high-resolution vibrational studies to the future extended-range electronic structural investigations.

III. RESULTS AND DISCUSSION

A. Electron irradiation on CO/Cu(100)

In Fig. 3, we show the effects of low-energy electron irradiation on CO/Cu(100). In particular, a typical vibrational EELS spectrum for 100 L (1 L = 1×10^{-6} Torr second) of CO on Cu(100) at 120 K is shown in Fig. 3(a). The characteristic peaks for ν(Cu–CO) at 338 cm^{-1} and ν(C–O) at 2084 cm^{-1} were found to be in good accord with previously published data.[1–3] The c(2×2)CO/Cu(100) sample was then irradiated with electrons (thermionically emitted from a heated tungsten filament positioned 40 mm from it at a typical flux of 2.7 μA/mm^2) at 100 eV IE for 10 minutes. After the electron irradiation, the c(2×2) LEED pattern was found to be less sharp, and the corresponding AES analysis revealed no discernible change in the small intensities of the C and O *KLL* Auger peaks at 272 eV and 503 eV, respectively. The ν(C–O) peak for the electron-irradiated sample remained at the same energy loss position [Fig. 3(b)] but with a reduction

in intensity[13] that was likely the result of electron-induced desorption and dissociation. On the other hand, the corresponding ν(Cu–CO) peak at 338 cm^{-1} became a broad shoulder, and could be attributed to an additional contribution from the well-known Cu–O stretch at 305 cm^{-1} as was previously observed for c(2×2)O/Cu(100).[14] When the sample temperature was slowly increased from 120 K, the peak at 2084 cm^{1} was found to gradually diminish [Fig. 3(c)] and to disappear at 200 K [Fig. 3(d)], revealing the peak at 2011 cm^{-1}. At this point, the LEED pattern became a diffused 1 ×1. The observed intensity reduction of the ν(C–O) peak at 2084 cm^{-1} with increasing temperature was consistent with previous work.[1] The new feature at 2011 cm^{-1} was clearly the result of low-energy electron irradiation and was tentatively attributed to a ''perturbed'' C–O stretch [i.e., a redshifted ν(C–O)]. After the electron-irradiated sample was annealed to 160 K, the broad shoulder at ~338 cm^{-1} became a single peak at 310 cm^{-1}, which could be assigned to the Cu–O stretch,[14] indicating the presence of atomic oxygen on the surface. The intensity of the peak at 2011 cm^{-1} remained essentially unchanged upon annealing to 370 K [Fig. 3(e)] and then decreased almost completely upon further annealing to 420 K [Fig. 3(f)]. In contrast, the peak at 310 cm^{-1} diminished in intensity gradually upon annealing from 160 K [Fig. 3(c)] to 420 K [Fig. 3(f)].

Additional experiments to further elucidate the nature of this redshifted ν(C–O) peak give the following results. (1) Reducing the electron IE from 100 to 40 eV appeared to have no significant effect on the corresponding EELS spectra, which indicates that an electron IE of 40 eV was sufficient to activate the surface reactions that generated the ''stabilized'' CO. (2) Exposing a high dose (1200 L) of CO to an amorphous Cu surface [obtained by sputtering Cu(100) in 2 ×10^{-5} Torr of Ar for 20 minutes at 500 eV IE] at 120 K and then annealing it to RT without electron irradiation did not produce the redshifted CO peak (at 2011 cm^{-1}). Since Ar^{+} sputtering is believed to introduce defect sites on Cu(100), this observation indicates that the presence of ''stabilized'' CO was not due to adsorption on defect sites. (3) Exposing CO to an oxygen-covered Cu(100) surface [which was prepared by exposing a clean Cu(100) surface at RT with different dosages of O_2 ranging from 0.5 to 300 L] at 120 K without electron irradiation and then annealing the resulting sample to RT did not generate the redshifted CO peak. This result indicates that without electron irradiation CO could neither adsorb on an ''oxidized'' Cu(100) surface nor coadsorb with surface oxygen atoms to produce the ''stabilized'' CO. Finally, (4) exposing CO to a carbon-covered Cu(100) surface [obtained by sputtering Cu(100) in C_2H_4 at RT and then annealing to 600 K] at 120 K without electron irradiation and then annealing the resulting sample to RT also did not produce the redshifted CO peak. This observation suggests that the redshifted CO peak was not caused by coadsorption of CO with the surface carbon.

All these experiments suggest that the observed redshifted peak at RT was due to ''stabilized'' CO species that were generated *in situ* during CO exposure by electron irradiation.

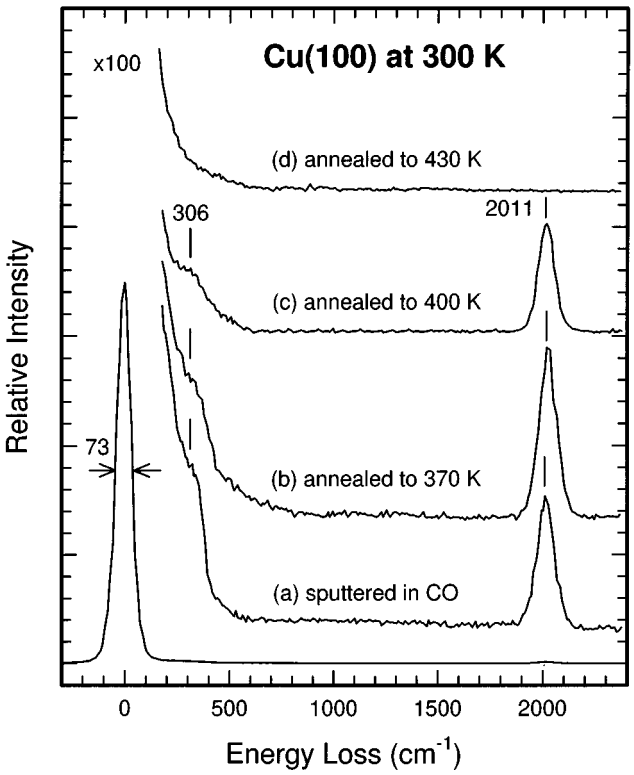

FIG. 4. Vibrational electron energy loss spectra for (a) Cu(100) sputtered in 1 × 10^{-6} Torr of CO at 200 eV and 10 nA/mm^2 for 10 minutes at 300 K, followed by annealing to (b) 370, (c) 400, and (d) 430 K.

We believe that irradiation by low-energy electrons alone has only minor effects on the surface itself. Indeed, no change in the (1×1) LEED pattern of a clean Cu(100) surface was observed for an extended period of irradiation with electrons below 100 eV. With electron irradiation at a higher IE (500 eV), the change in the sharpness of the LEED pattern of the resulting sample was also not readily discernible, which suggests that electron irradiation even at this high energy did not significantly roughen the surface. The presence of ''stabilized'' CO generated at the lower electron IE was therefore not due to adsorption on defect sites. Furthermore, despite the redshift of 73 cm^{-1} from its nominal low-temperature position at 2084 cm^{-1}, the vibrational peak at 2011 cm^{-1} could only be assigned to the stretch frequency of a triply bonded C–O on an atop site, because adsorption of a doubly bonded CO at a bridge site[15] (or a four-fold hollow site) would give rise to vibration at a considerably lower frequency.

B. Ion irradiation of Cu(100) in CO at RT

The RT adsorption of CO on Cu(100) could also be obtained by low-energy ion irradiation of Cu(100) in CO at RT. Figure 4(a) shows the presence of the ν(C–O) peak at 2011 cm^{-1} for a Cu(100) surface sputtered at RT in 1×10^{-6} Torr of CO for 10 minutes at an ion IE of 200 eV. A diffused (1 ×1) LEED pattern was observed for the resulting sample. Furthermore, the redshifted CO peak became more intense as

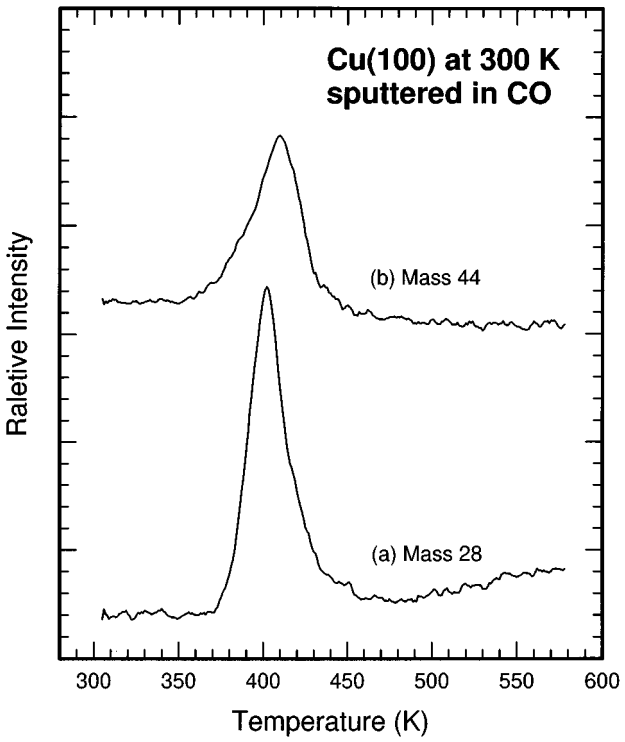

FIG. 5. TPD profiles of (a) mass 28 and (b) mass 44 for Cu(100) sputtered in 1×10^{-6} Torr of CO at 200 eV and 10 nA/mm^2 for 10 minutes at 300 K. The linear heating rate was 1 K/s.

the sample was annealed from RT [Fig. 4(a)] to 370 K [Fig. 4(b)]. It became weaker upon further annealing to 400 K [Fig. 4(c)] and finally disappeared at 430 K [Fig. 4(d)]. The corresponding TPD profiles show that the desorption maxima for mass 28 [corresponding to CO, in Fig. 5(a)] and mass 44 [corresponding to CO_2, in Fig. 5(b)] occurred near 400 K. The temperature of the desorption maximum observed in the TPD experiment [Fig. 5(a)] is therefore consistent with the EELS results (Fig. 4). In addition to the presence of CO, the presence of CO_2 can be explained by the CO oxidation reaction with surface oxygen [i.e., CO (ad) + O (ad) $\rightarrow$ CO_2 (gas)]. In comparison with the results of the electron irradiation experiment (Sec. III A), the adsorption feature obtained by ion irradiation in CO was found to have the same vibrational frequency (2011 cm^{-1}) and the same desorption maximum (400 K). These similarities strongly suggest that both electron irradiation and ion irradiation in CO generated the same kind of ''stabilized'' CO adsorption.

Along with the reaction activation process, additional effects due to sputtering and defect-site creation were also introduced during the ion irradiation process. In general, the rate of radiation damage on the sample depends on many factors, including the kinetic energy and mass of the ion, the substrate temperature, and the nature of the material.[16] Unlike electron irradiation, irradiation with ions at 50 eV was found to be sufficient to cause a diffused LEED pattern and the intensity of the elastic peak in the EELS spectrum to decrease significantly, both of which are indicative of radiation damage on the sample. In order to isolate the reaction activation effect from the substrate damage effect, we have repeated the experiments with different ion IEs from 50 to 500 eV. These studies showed that the intensity of the CO peak at 2011 cm^{-1} increased slowly with increasing ion IE. However, when CO was directly exposed to an amorphous surface (obtained by sputtering in 2×10^{-5} Torr of Ar for 10 minutes at 500 eV ion IE) without *in situ* ion irradiation during dosing, the redshifted CO peak was not observed. Furthermore, exposing CO at 50 eV ion IE on the amorphous surface did not produce a stronger redshifted CO peak than that on a clean Cu(100) surface. The redshifted CO peak could not therefore be attributed to adsorption on defect sites. The slow increase in the intensity of the redshifted CO peak with increasing ion IE was related to variation in the ion flux caused by changes in the focusing conditions of the ion beam when the IE was varied. On the other hand, increasing the irradiation time from 1 to 10 minutes caused the peak intensity at 2011 cm^{-1} to increase correspondingly. The increase in the peak intensity leveled off upon a further increase in the irradiation time from 10 to 30 minutes, indicating the onset of an equilibrium condition between the reaction rate and the rate of adsorbate removal.

C. Ion irradiation of Cu(100) in C_2H_4 with pre- and postexposure of O_2 at RT

Like CO, C_2H_4 was found to adsorb on Cu(100) only at low temperature.[17] However, our AES results indicated the presence of surface carbon after the clean Cu(100) surface was exposed to 600 L of C_2H_4 at RT with ion irradiation at a low ion IE of 50 eV. At a higher dose (5000 L) of C_2H_4 with ion irradiation, our EELS results indicated the adsorption of CH fragments.[18] Based on these exposure studies, we used a relatively low dose (600 L) of C_2H_4 with ion irradiation in order to generate surface carbon to investigate its reaction with atomic oxygen pre-deposited on the surface. It should be noted that an oxygen-covered Cu(100) surface can be obtained by directly dosing O_2 to Cu(100) at RT.[14] Figure 6 shows the EELS spectrum for an O-pre-covered Cu(100) sample ion irradiated in 1×10^{-6} Torr of C_2H_4 at 50 eV for 10 minutes at RT. For a 500 L pre-exposure of O_2 to Cu(100) at RT, we found the characteristic ν(Cu–O) peak at 300 cm^{-1} and a c(2×2) LEED pattern, which are consistent with the dissociative adsorption of O_2 observed in the previous work.[14] Evidently the energy loss peak at 2011 cm^{-1}, characteristic of the previously observed ''stabilized'' CO adsorption, could again be obtained by ion irradiation of the oxidized sample in C_2H_4 at RT [Fig. 6(b)]. This peak became more intense as the sample was annealed from RT to 370 K [Fig. 6(c)] and then almost completely diminished upon further annealing to 430 K [Fig. 6(d)].

The presence of the redshifted CO peak did not appear to depend on the order of dosing O_2 and ion irradiation in C_2H_4 (Fig. 7). Despite the lack of any discernible feature in the EELS spectrum for a clean Cu(100) surface after ion irradiation in C_2H_4 at 50 eV IE [Fig. 7(a)], the corresponding AES result clearly indicated an increase in the surface carbon concentration. After 100 L of O_2 was subsequently exposed

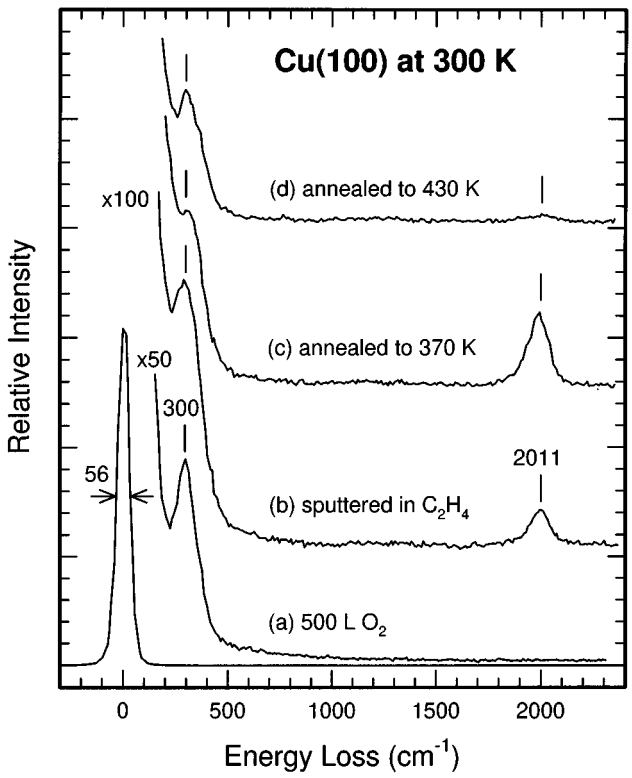

FIG. 6. Vibrational electron energy loss spectra for (a) Cu(100) exposed with 500 L of O_2 at 300 K, and (b) sample (a) sputtered in 1×10^{-6} Torr of ethylene at 50 eV and 10 nA/mm^2 for 10 minutes, followed by annealing to (c) 370 and (d) 430 K.

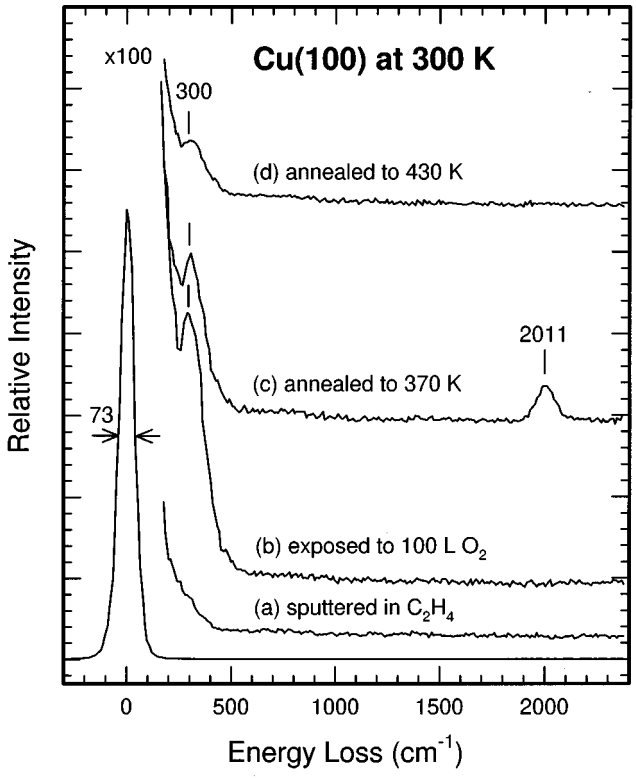

FIG. 7. Vibrational electron energy loss spectra for (a) Cu(100) sputtered in 1×10^{-6} Torr of ethylene at 50 eV and 10 nA/mm^2 for 10 minutes at 300 K, and (b) sample (a) exposed with 100 L of O_2, followed by annealing to (c) 370 and (d) 430 K.

to the surface [Fig. 7(b)], a prominent ν(Cu–O) peak at 300 cm^{-1} was observed. When the sample was annealed to 370 K [Fig. 7(c)], the CO peak at 2011 cm^{-1} reappeared and could again be removed by annealing it to 430 K. In keeping with the EELS results shown in Figs. 6 and 7, the corresponding TPD data revealed that maximum desorption of both CO and CO_2 from the surface occurred near 400 K, which is similar to the results shown in Fig. 5. Apparently, the peak at 2011 cm^{-1} in Figs. 6 and 7 can be attributed to the same ''stabilized'' CO adsorption observed earlier. On the other hand, if the C-covered surface [Fig. 7(a)] was annealed to 500 K first and then followed by O_2 exposure at RT, no redshifted CO peak was observed even upon annealing the sample to 370 K. This indicates that the presence of surface atomic carbon (and/or C-containing fragments) produced by ion irradiation in C_2H_4 was essential to the formation of the redshifted CO peak. As the C-covered sample was annealed to 500 K, the carbon atoms either combined with one another to form graphite or diffused into the bulk, preventing the formation of the ''stabilized'' CO species on Cu(100). Since the deposition of surface carbon was achieved by ion irradiation in the present experiment, the effect of defect sites cannot be ruled out. However, the results of the other experiments shown in Sections III A and III B argue against the formation of ''stabilized'' CO caused by these defect sites.

In summary, the formation of ''stabilized'' CO may be considered as a two-step process: (1) reactant formation of surface C by EII in CO or C_2H_4, and of surface O by EII in CO or by directly exposing O_2 to the sample at RT; and (2) *in situ* surface reaction between the adsorbed C and O reactants following the equation: C (ad) + O (ad) $\rightarrow$ CO (ad) during EII or by thermal annealing to 370 K.

D. Bonding model for the ''stabilized'' CO adsorption

It is well known that chemisorption of CO on Cu(100) is extremely weak. To the best of our knowledge, the present work reports the first observation of CO adsorption on Cu(100) at RT. Furthermore, the apparent stabilization of CO at RT is characterized by a redshift of 73 cm^{-1} in the ν(C–O) peak observed for the adsorption of CO on Cu(100) at low temperature. Although we cannot rule out the defect-site effect, the experiments involving electron irradiation and an amorphous surface provide no evidence to support the conjecture that the ''stabilized'' CO adsorption was caused by defect sites. Since CO has not been previously observed on other types of adsorption sites except for the atop site on Cu(100), an adsorption geometry based on terminally bonded CO remains our favorite choice to account for the observed ''stabilized'' structure at RT. In particular, the ν(C–O) value for the bridge sites is expected to be considerably lower than 2011 cm^{-1}. For example, a frequency of 1882 cm^{-1} has been attributed to the vibrational feature of a proposed Cu_2CO species that involves a CO molecule bridge bonded to two Cu atoms.[15] No report of CO adsorbed on a

four-fold hollow site of Cu(100) is available in the literature. On the other hand, a redshift of 73 cm^{-1} is too large to be caused by adsorption on different low Miller index planes of Cu, because the previous studies have shown that the ν(C–O) frequencies for Cu(111) and Cu(110) could at most differ from that for Cu(100) by 15–24 cm^{-1}.[19] Since a new or additional bonding structure is needed to stabilize CO on the Cu(100) surface, the most likely mechanism is coadsorption. Although no direct evidence is found to support the presence of C (and hence its coadsorption with CO), the coadsorption of CO with O is plausible due to the presence of O on the surface, as indicated by the ν(Cu–O) peak in the EELS spectrum and by the corresponding TPD profiles (of CO and CO_2).

There have been many studies on the coadsorption of promoters and inhibitors with CO on fcc metal surfaces. In particular, it has been shown that the ν(C–O) frequency can be reduced (redshifted) by the coadsorption of such promoters as Na (Ref. 20) and K.[21] On the other hand, the coadsorption of CO with inhibitors such as O was found to induce both red- and blueshifts in the ν(C–O) frequency.[22,23] There are at least five mechanisms that have been proposed to explain the ν(C–O) frequency shifts induced by coadsorption:[24] (1) the indirect surface-mediated interaction, (2) the direct coadsorbate-to-CO interaction, (3) adsorption geometry and related effects, (4) sp^2 rehybridization, and (5) the surface image charge effect. The most popular models involve indirect and direct interactions. The indirect interaction model is based on electron transfer between the coadsorbate and the $2\pi^*$ antibonding orbital of a neighboring CO molecule through the *d* orbitals of the metal substrate. In this model, a promoter donates electrons to the metal surface usually through a dative σ bond, which results in an upward shift of the Fermi level and hence increases the electron back donation from the metal to the $2\pi^*$ orbital of CO. Since the antibonding between the CO molecule and the metal is enhanced, the C–O triple bond is concomitantly weakened, which gives rise to a redshift in the ν(C–O) frequency. However, when CO coadsorbs with an inhibitor that withdraws electrons from the metal surface, the back donation to the $2\pi^*$ orbital is reduced and the C–O triple bond is strengthened, resulting in a blueshift. In our case, if CO were to coadsorb with O, a blueshifted ν(C–O) feature would be expected. The lack of any discernible blueshifted feature therefore suggests that the surface-mediated interaction does not play a significant role. On the other hand, the overlap between a coadsorbate orbital and the $2\pi^*$ orbital of CO in the direct interaction model would lead to the formation of a coadsorbate-CO quasicomplex. In effect, the electron delocalization of the C–O multiple bond density to a coadsorbed O atom causes the C–O bond to weaken, inducing a redshift in the ν(C–O) frequency. In this model, the proposed O–CO quasicomplex can be used to explain the redshift observed in our experiments. In particular, an orbital from O overlaps with the $2\pi^*$ orbital of CO to form a partial bond, which reduces the bond order of CO and gives rise to a redshift in the ν(C–O) frequency. In the case of possible geometry-related effects, an earlier infrared study on the interactions of CO adsorbed on oxygen-pre-covered Cu(111) and Cu(110) surfaces[23] has revealed a doublet structure near 2110 cm^{-1}, which was proposed to be caused by different bonding sites. In contrast, our studies do not find any change in the ν(C–O) frequency upon different exposures of oxygen and under different ion irradiation conditions, which suggests that the bonding-site effect does not cause the observed frequency shift. Finally, we cannot rule out the contribution due to electrostatic interaction between the permanent dipole of CO and the dipole generated by a coadsorbate and its surface image charge, because of the unknown magnitude of the dipole interaction involved.

Given the observed redshift, we favor a direct-interaction bonding model involving an O–CO quasicomplex. In particular, the unusual stabilization of CO adsorption found in our experiments can be explained by a partial bond between a CO molecule adsorbed on an atop site and a coadsorbed O atom. Furthermore, a calculated potential energy surface for the ground state of CO_2 suggests that a ''free'' CO_2 molecule dissociates into CO and O at an O-to-CO separation of $\sim$2.2 Å.[25] The proposed direct interaction between CO and O must therefore involve an O-to-CO separation smaller than 2.2 Å. In the commonly accepted terminally bonded adsorption model for CO on Cu(100),[4] this separation can only be realized if CO is slightly tilted towards the coadsorbed O atom. Since earlier studies for O on Cu(100) have demonstrated that O adsorbs in a four-fold hollow site,[14] a plausible bonding structure therefore involves the stabilization of a terminally bonded CO molecule, slightly tilted at the atop site, by a coadsorbed O atom in a nearest-neighbor four-fold hollow site (Fig. 8). The lack of any direct evidence for the vibration of the coadsorbed-O-to-CO bond in the EELS experiments is consistent with the weak dipole intensity of a nearly surface-parallel bond.

Finally, in addition to the coadsorption-induced shift, a coupling shift and a chemical shift may also occur. It was shown that on a clean Cu(111) surface the nearly constant value for the ν(C–O) frequency observed at different CO coverages is a consequence of the interplay between two large but opposing effects: a coupling shift that tends to increase the frequency with increasing coverage and a chemical shift that tends to reduce it.[26] The frequency shifts induced by these effects are, however, usually smaller than 40 cm^{-1} individually and even smaller when the two effects are combined. They are therefore not expected to play an important role for the 73 cm^{-1} redshift found in the present case.

IV. CONCLUDING REMARKS

In the present work, we have investigated the effects of low-energy electron or ion irradiation on the adsorption of CO on Cu(100) using high-resolution EELS and TPD techniques. Unusually stable CO adsorption on Cu(100) at RT was found as a result of a surface reaction: C (ad) + O (ad) $\rightarrow$ CO (ad), whereby the atomic reactants C and O were produced *in situ* by electron irradiation of CO/Cu(100) or by ion irradiation of Cu(100) in CO or in C_2H_4 with pre- and

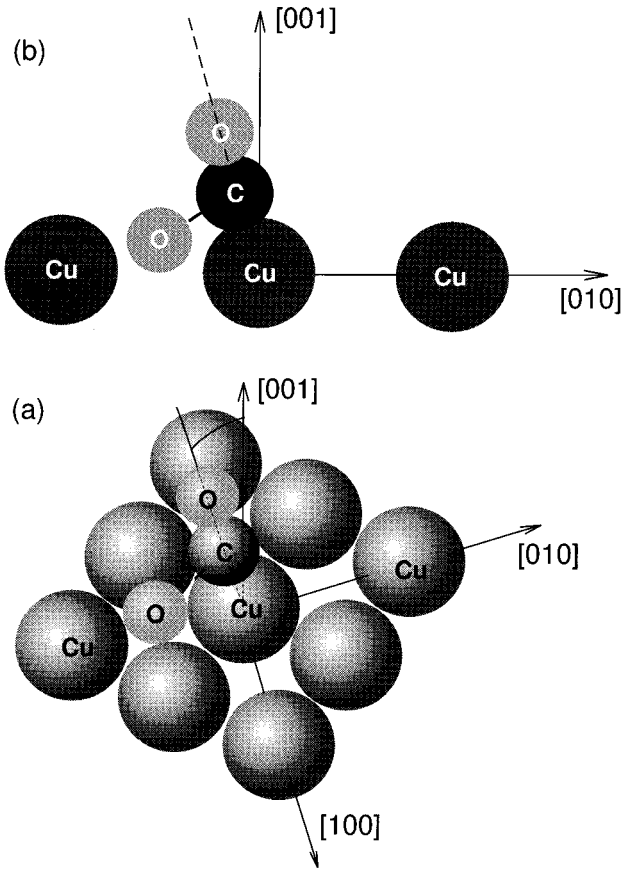

FIG. 8. Perspective (a) and side view (b) diagrams of a proposed bonding structure for CO coadsorbed with O on Cu(100).

postexposure of O_2. In particular, CO adsorption was found to be stabilized on Cu(100) at a temperature as high as 420 K, and was characterized by a redshift of 73 cm^{-1} in the nominal ν(C–O) frequency (observed at low temperature). Different possible effects induced by electron or ion irradiation were considered. To explain the observed redshift and stabilization effects, we propose a bonding model that involves direct interaction between a CO molecule on an atop site and a coadsorbed O atom in a neighboring four-fold hollow site. The present work therefore not only provides direct evidence for CO production at RT by electron- and ion-induced surface reactions on an ''unreactive'' surface such as Cu(100), but also illustrates the importance of coadsorbed surface O on practical surface reactions. It further demonstrates the enormous potential of activating surface reactions by means of low-energy electron or ion irradiation and the effectiveness of studying this type of systems by using standard surface analysis methods such as EELS and TPD.

ACKNOWLEDGMENTS

This work was supported by the Natural Sciences and Engineering Research Council of Canada. It is the authors' pleasure to thank Jacek Szubra and the entire staff of the Science Shops for their skillful workmanship in the development of their EELS machine.

[1]S. Andersson, Surf. Sci. **89**, 477 (1979).
[2]S. Andersson and B. N. J. Persson, Phys. Rev. Lett. **45**, 1421 (1980); Phys. Rev. B **24**, 3659 (1981).
[3]B. A. Sexton, Chem. Phys. Lett. **63**, 451 (1979).
[4]S. Andersson and J. B. Pendry, Phys. Rev. Lett. **43**, 363 (1979).
[5]B. A. Sexton, Surf. Sci. **88**, 299 (1979).
[6]D. L. Smith, *Thin Film Deposition Principles and Practice* (McGraw-Hill, New York, 1995), Chap. 8.
[7]M. H. Mohamed and L. L. Kesmodel, Surf. Sci. Lett. **185**, L467 (1987).
[8]Edited by J. J. Cuomo, S. M. Rossnagel, and H. R. Kaufman, *Handbook of Ion Beam Processing Technology* (Noyes, Park Ridge, NJ, 1989).
[9]D. Q. Hu, Ph.D. thesis, University of Waterloo, Waterloo, Canada (1993).
[10]H. Ibach and D. L. Mills, *Electron Energy Loss Spectroscopy and Surface Vibrations* (Academic, New York, 1982); H. Ibach, *Electron Energy Loss Spectrometers*, Springer Series in Optical Science Vol. 63 (Springer, New York, 1991).
[11]S. D. Kevan, Rev. Sci. Instrum. **54**, 1441 (1983).
[12]A. Spitzer and H. Luth, Surf. Sci. **102**, 29 (1981).
[13]It should be noted that differences in the changes in the C and O intensities observed using AES and EELS are due to the differences in the surface sensitivity of each technique. In our case, EELS is considerably more surface sensitive than AES.
[14]M. Wuttig, R. Franchy, and H. Ibach, J. Electron Spectrosc. Relat. Phenom. **44**, 317 (1987), and references therein.
[15] M. Moskovits and J. E. Hulse, J. Phys. Chem. **81**, 2004 (1977).
[16]J. E. Greene, S. A. Barnett, J. E. Sundgren, and A. Rockett, in *Ion Beam Assisted Film Growth*, edited by T. Itoh (Elsevier, Amsterdam, 1989), p. 101.
[17]C. Nyberg, C. G. Tengstal, and S. Andersson, Chem. Phys. Lett. **87**, 87 (1982).
[18]H. Yu and K. T. Leung, Surf. Sci. (to be published).
[19]K. Horn, M. Hussian, and J. Prichard, Surf. Sci. **63**, 244 (1977), and references therein.
[20]L. Wallden, Surf. Sci. Lett. **134**, L513 (1983).
[21]L. H. Dubois, B. R. Zegarski, and H. S. Luftman, J. Chem. Phys. **87**, 1367 (1987).
[22]W. K. Kuhn, J. W. He, and D. W. Goodman, in *Surface Science of Catalysis*, ACS Symposium Series, edited by D. J. Dwyer and F. M. Hoffman **482**, 71 (1992).
[23]P. Hollins and J. Pritchard, Surf. Sci. **134**, 91 (1983).
[24]G. Pacchioni and P. S. Bagus, Chem. Phys. **177**, 373 (1993).
[25]G. Herzberg, *Molecular Spectra and Molecular Structure* (Van Nostrand, Toronto, 1966), Vol. 3, p. 429.
[26]P. Hollins and J. Pritchard, Surf. Sci. **89**, 486 (1979).